Inorganic Chemistry

Article

pubs.acs.org/IC

Pd^{2+}-Incorporated Perovskite $CaPd_3B_4O_{12}$ (B = Ti, V)

Kentaro Shiro,[†] Ikuya Yamada,*[,†,‡,§] Naoya Ikeda,[†] Kenya Ohgushi,[∥,§] Masaichiro Mizumaki,[⊥,⊗] Ryoji Takahashi,[†] Norimasa Nishiyama,[○,#] Toru Inoue,[○] and Tetsuo Irifune[○]

[†]Department of Chemistry, Graduate School of Science and Engineering, Ehime University, 2-5 Bunkyo-cho, Matsuyama, Ehime 790-8577, Japan

[‡]Nanoscience and Nanotechnology Research Center, Osaka Prefecture University, 1-2 Gakuen-cho, Naka-ku, Sakai, Osaka 599-8570, Japan

[§]Transformative Research-Project on Iron Pnictides (TRIP), Japan Science and Technology Agency (JST), Chiyoda-ku, Tokyo 102-0075, Japan

[∥]Institute for Solid State Physics (ISSP), University of Tokyo, 5-1-5 Kashiwanoha, Kashiwa, Chiba 227-8581, Japan

[⊥]Japan Synchrotron Radiation Research Institute (JASRI), Sayo-cho, Sayo-gun, Hyogo 679-5198, Japan

[⊗]Core Research for Evolutional Science and Technology (CREST), JST, 5 Sanbancho, Chiyoda-ku, Tokyo 102-0075, Japan

[○]Geodynamics Research Center (GRC), Ehime University, 2-5 Bunkyo-cho, Matsuyama, Ehime 790-8577, Japan

Supporting Information

ABSTRACT: Novel A-site ordered perovskites $CaPd_3Ti_4O_{12}$ and $CaPd_3V_4O_{12}$ were synthesized under high-pressure and high-temperature of 15 GPa and 1000 °C. These compounds are the first example in which a crystallographic site in a perovskite-type structure is occupied by Pd^{2+} ions with a $4d^8$ low spin configuration. The ionic models for these compounds were determined to be $Ca^{2+}Pd^{2+}{}_3Ti^{4+}{}_4O_{12}$ and $Ca^{2+}Pd^{2+}{}_3V^{4+}{}_4O_{12}$ by structural refinement using synchrotron X-ray powder diffraction, hard X-ray photoemission, and soft X-ray absorption spectroscopy. Magnetic susceptibility, electrical resistivity, and specific heat measurements demonstrated diamagnetic insulating behavior for $CaPd_3Ti_4O_{12}$ in contrast to the Pauli-paramagnetic metallic nature of $CaPd_3V_4O_{12}$.

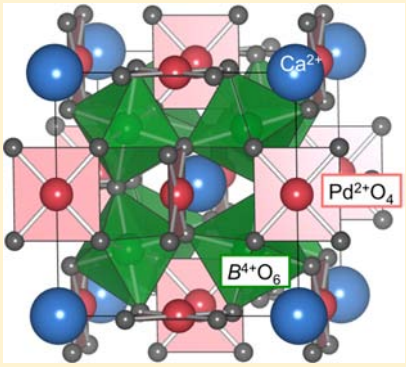

INTRODUCTION

Perovskite-type oxide ABO_3 and its derivatives are known to accommodate a wide range of metal elements because of the flexibility of their composition and structure. Among d-block metals, palladium is rarely incorporated into certain crystallographic sites in perovskite-type oxides at full occupancy. This is because the Pd^{2+} ion, which is the most common state in palladium oxide, usually has a $4d^8$ low spin (S = 0) electron configuration with a strong tendency to be placed in a square planar coordination with a large crystal field splitting, although there are a very small number of examples of Pd^{2+} ions in octahedral coordinations.[1] This is in contrast with the isoelectronic Ni^{2+} ion ($3d^8$), which occupies the octahedral B-site of ABO_3 perovskite in a high spin configuration (S = 1).[2,3] Pd^{3+} ion ($4d^7$), which can be generated using a highly oxidizing atmosphere, is unstable, and disproportionates into Pd^{2+} and Pd^{4+} ions. To the best of our knowledge, $LaPdO_3$ perovskite is the only compound in which Pd^{3+} ion fully occupies the B-site in the perovskite structure.[4]

Cation orderings of A-, B-, and both sites are known in perovskite and related structures. In quadruple A-site ordered perovskite, $AA'_3B_4O_{12}$ (Figure 1),[5] three-quarters of the A-sites (= A'-site) are of a pseudosquare planar coordination suited to Jahn−Teller active ions such as Cu^{2+} and Mn^{3+}, while the remaining quarter of A-sites are occupied by typical large A-site ions such as alkaline, alkaline earth, and rare earth metal ions.[6−8] All attempts to replace Cu^{2+} with Pd^{2+} at the A'-site failed at ambient pressure,[9] although this site is also expected to be suitable for Pd^{2+} ions. Recent exploratory studies on perovskite oxides have shown that high-pressure and high-temperature treatment may work effectively to stabilize the $AA'_3B_4O_{12}$-type perovskite structure for a variety of constituent elements. Substitutions of A'-site cation with non-Jahn−Teller ions such as Fe^{2+} and $Mn^{1.67+}$ were successful using high-pressures of approximately 10 GPa.[10,11] Hence, we tentatively adopted high-pressures of up to 15 GPa to substitute Pd^{2+} for Cu^{2+} in $CaCu_3B_4O_{12}$ (B = Ti or V) perovskites.

In this paper, we report the high-pressure synthesis of novel A-site ordered perovskites $CaPd_3Ti_4O_{12}$ (CPTO) and $CaPd_3V_4O_{12}$ (CPVO), in which the A'-sites are entirely occupied by Pd^{2+} ions. Spectroscopic investigations revealed that the valence states of these perovskites are $Ca^{2+}Pd^{2+}{}_3Ti^{4+}{}_4O_{12}$ and $Ca^{2+}Pd^{2+}{}_3V^{4+}{}_4O_{12}$. From structure

Received: November 17, 2012
Published: January 18, 2013

   dx.doi.org/10.1021/ic3025155 | Inorg. Chem. 2013, 52, 1604−1609

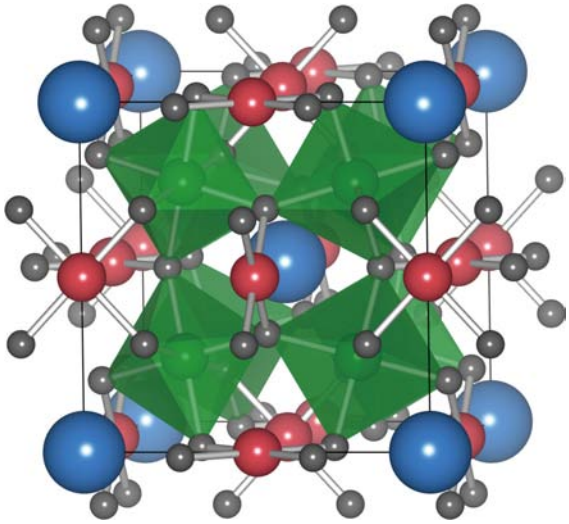

Figure 1. Crystal structure of $AA'_3B_4O_{12}$-type perovskite. The blue (A), red (A'), green (B), and gray (O) spheres represent the relevant atoms. The unit cell is built up by the atoms inside the solid lines: eight distorted BO_6 octahedra that are tilted relative to one another, A' ions bonded to four closest oxygen atoms, and A ions at the corners and the body-center (bonds not shown).

refinement based on synchrotron X-ray powder diffraction (SXRD), we found that the metal−oxygen angles are primarily dependent on the difference between the A'- and A-site ion sizes for $AA'_3B_4O_{12}$-type perovskite structure. Magnetic property, electrical resistivity, and specific heat measurements revealed CPTO to be a diamagnetic insulator and CPVO to be a Pauli-paramagnetic metal.

EXPERIMENTAL SECTION

Polycrystalline samples of CPTO and CPVO were synthesized under high-pressure and high-temperature conditions. Stoichiometric mixtures of CaO (99.9%, Rare metallic), PdO (99.9%, Rare metallic), and TiO_2 (99.9%, Rare metallic) or VO_2 (99.9%, Rare metallic) were ground in an agate mortar, and then placed into a gold capsule (2.8 mm diameter and 4.0 mm high). The capsule was set in a graphite furnace within a MgO high-pressure medium. The above procedures were conducted in a nitrogen-filled glovebox because of the hygroscopic nature of CaO. The high-pressure medium was framed by WC anvils and compressed to 10−15 GPa using a Kawai-type high-pressure apparatus at GRC, Ehime University. We used the graphite furnace to heat the sample at 1000 °C for 30 min, while retaining the high-pressure. This was followed by quenching to room temperature, and then slowly releasing the pressure.

Phase identification was made from the X-ray powder diffraction (XRD) pattern collected using a Rigaku MiniFlex II diffractometer with Cu $K\alpha$ radiation. SXRD data were collected using a Debye−Scherrer camera installed at the BL02B2 beamline at SPring-8. The powder samples were sealed in Lindemann glass capillaries with an inner diameter of 0.2 mm. The wavelength was calibrated as 0.51764 Å using a CeO_2 standard. Crystal structure refinement was performed based on the SXRD data using the Rietveld program RIETAN-FP.[12] In the refinement, the absorption correction was not made.

Hard X-ray photoemission spectroscopy (XPS) measurements were carried out using the VG-SCIENTA R-4000 spectrometer installed at the BL47XU beamline at SPring-8. The incident photon energy was 7.94 keV. The XPS spectra of the inner-shell electrons of Pd 3d, Ti 2p, and V 2p were collected at 300 K. The energy scale was calibrated using the Fermi edge of a deposited gold sample. The energy resolution of this system is about 280 meV around 7.94 keV. Soft X-ray absorption spectroscopy (XAS) measurements were conducted using a total electron yield method at the BL27SU beamline at SPring-8. Ti $L_{2,3}$-edge, and V $L_{2,3}$-edge XAS spectra were collected at 300 K. The energy resolution, $\Delta E/E$, was greater than 5000.

Electrical resistivity measurements were carried out between 5 and 300 K using a standard four-probe method (PPMS, Quantum Design). The temperature dependence of the magnetic susceptibility was measured with both zero-field cooling (ZFC) and field cooling (FC) modes between 5 and 300 K in an external field of 1 kOe using a superconducting quantum interference device magnetometer (MPMS-XL, Quantum Design). Heat capacity measurements were performed using a conventional relaxation method (PPMS, Quantum Design).

RESULTS AND DISCUSSION

No trace of a perovskite phase was found in the XRD patterns of the CPTO samples synthesized at pressures up to and including 12 GPa, whereas a cubic $AA'_3B_4O_{12}$-type perovskite phase (space group $Im\bar{3}$, No. 204) was identified as the major phase for the samples synthesized at 15 GPa. This indicates that a high-pressure of about 15 GPa is necessary to stabilize CPTO perovskite phase, although the isostructural $CaCu_3Ti_4O_{12}$ can be synthesized by solid state reaction under ambient pressure.[6] The difference in the synthesis conditions needed for CPTO and $CaCu_3Ti_4O_{12}$ is probably because of the larger ionic radius of Pd^{2+} ion (Shannon's ionic radius, 0.64 Å) compared with that of Cu^{2+} ion (0.57 Å).[13] High-pressure conditions could stabilize such a large ion at the A'-site, being in agreement with the previous report that the isostructural $CaFe_3Ti_4O_{12}$ phase with Fe^{2+} ion (0.64 Å)[13] at the A'-site was synthesized at pressures over 7 GPa.[10]

The best quality samples of CPTO and CPVO were obtained using high-pressure and high-temperature conditions of 15 GPa and 1000 °C. Figure 2 shows the SXRD patterns and Rietveld refinement results for these compounds. The Bragg reflections of the main phase were indexed as $AA'_3B_4O_{12}$-type perovskites with a = 7.49777(14) Å for CPTO and a = 7.40317(8) Å for CPVO. Small amounts (estimated as several wt %) of impurities including unidentified phase(s) were found for both compounds. We selected appropriate initial structure models for the Rietveld refinement of CPTO and CPVO based on the following considerations. A certain amount of substitution of A'-site ion with B-site ion was reported in this type of perovskite: for example, the Jahn−Teller-active Mn^{3+} ion occupies the A'-site for $Ca(Cu,Mn)_3Mn_4O_{12}$,[14] and partial substitution of Cu^{2+} with Ti^{4+} was reported in $Na(Cu^{2+}_{2.5}Ti^{4+}_{0.5})Ti_4O_{12}$,[15] which is required to retain the charge balance. However, it is unlikely that a significant amount of Ti^{4+} ions are incorporated into the A'-site for CPTO, because the starting composition in this study did not deviate from the stoichiometric composition. The Pd^{2+} ion is also unlikely to occupy the octahedral B-site because of the strong preference of the low spin d^8 electron configuration for square coordination. Hence, the structure model in which the respective A'- and B-sites are entirely occupied by Pd^{2+} and Ti^{4+} ions is reasonable as the first approximation. This approximation was also used for CPVO, based on the same considerations. As shown later, XPS and XAS spectra revealed that there is no indication of oxygen deficiency that would cause deviation of the metal valences from the stoichiometric ion models. Thus, we adopted models with stoichiometric compositions for both CPTO and CPVO. The reliability factors R_{wp} and R_B, and the goodness-of-fit S_{fit}, indicate satisfactory structure refinement results based on the stoichiometric composition model (R_{wp} = 5.770%, R_B = 3.432%, and S_{fit} = 1.302 for CPTO and R_{wp} = 6.560%, R_B = 2.047%, and S_{fit} = 1.631 for CPVO). Table 1 lists the refined structure parameters, selected bond lengths, and bond valence

dx.doi.org/10.1021/ic3025155 | Inorg. Chem. 2013, 52, 1604−1609

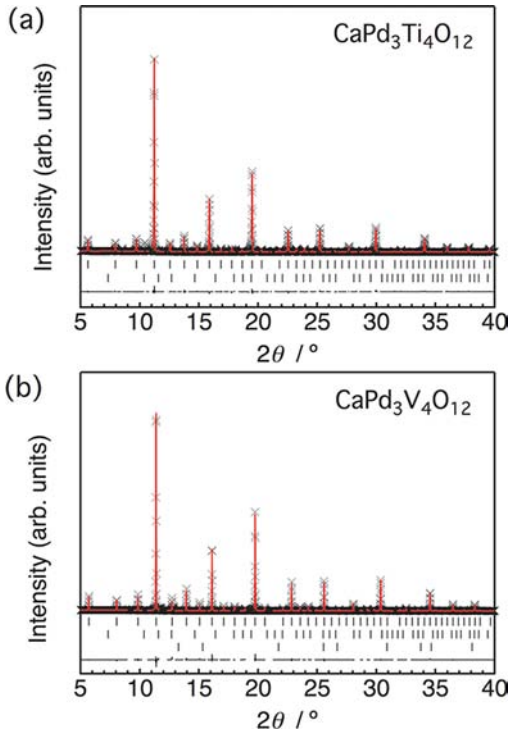

Figure 2. SXRD patterns and Rietveld refinement results for (a) $CaPd_3Ti_4O_{12}$ and (b) $CaPd_3V_4O_{12}$. The markers and lines indicate the observed and calculated profiles, respectively. Vertical marks show the positions of Bragg reflections for the perovskite phase and the impurity phases: $CaPd_3O_4$ (~0.6 wt %) for $CaPd_3Ti_4O_{12}$; and $CaPd_3O_4$ (~1 wt %), and Pd (~0.05 wt %) for $CaPd_3V_4O_{12}$, in order from top to bottom. The differences between the observed and calculated patterns are shown at the bottom.

Table 1. Refined Structure Parameters, Selected Bond Lengths, and BVS of Each Metal Ion for $CaPd_3Ti_4O_{12}$ and $CaPd_3V_4O_{12}$.[a]

	$CaPd_3Ti_4O_{12}$	$CaPd_3V_4O_{12}$
a/Å	7.49777(14)	7.40317(8)
x (O)	0.2961(4)	0.2947(3)
y (O)	0.1859(3)	0.1856(3)
B(Ca)/Å^2	0.47(5)	0.79(4)
B(Pd)/Å^2	0.661(14)	0.275(12)
B(Ti/V)/Å^2	0.3[b]	0.315(15)
B(O)/Å^2	0.45(5)	0.8[b]
Ca−O (×12)/Å	2.621(3)	2.5785(2)
Pd−O (×4)/Å	2.069(3)	2.0487(2)
Pd−O (×4)/Å	2.808(3)	2.7798(2)
Ti/V−O (×6)/Å	1.9658(7)	1.9397(7)
BVS(Ca)	2.05	2.30
BVS(Pd)	2.15	2.28
BVS(Ti/V)	3.99	3.94

[a]Space group: $Im\bar{3}$ (No.204); atomic sites: Ca 2*a* (0, 0, 0), Pd 6*b* (0, $^1/_2$, $^1/_2$), Ti/V 8*c* ($^1/_4$, $^1/_4$, $^1/_4$), O 24*g* (*x*, *y*, 0); R_{wp} = 5.770%, R_B = 3.432%, and S_{fit} = 1.302 for $CaPd_3Ti_4O_{12}$, R_{wp} = 6.560%, R_B = 2.047%, and S_{fit} = 1.631 for $CaPd_3V_4O_{12}$. The occupancy factor *g* for all sites was fixed at unity. [b]Isotropic atomic displacement parameters were fixed at typical values for Ti 8*c* site of $CaPd_3Ti_4O_{12}$ and O 24*g* site of $CaPd_3V_4O_{12}$.

sums (BVS)[16] calculated from the structure parameters for CPTO and CPVO. The BVS for Ca (+2.05), Pd (+2.15), and Ti (+3.99) suggest an ionic model of $Ca^{2+}Pd^{2+}{}_3Ti^{4+}{}_4O_{12}$. For CPVO, the BVS for Ca (+2.30), Pd (+2.28), and V (+3.94) imply an ionic model of $Ca^{2+}Pd^{2+}{}_3V^{4+}{}_4O_{12}$.

The valence states of the constituent metals of CPTO and CPVO perovskites were examined using XPS and XAS. Figure 3a shows the Pd 3d XPS spectra of CPTO and CPVO. The

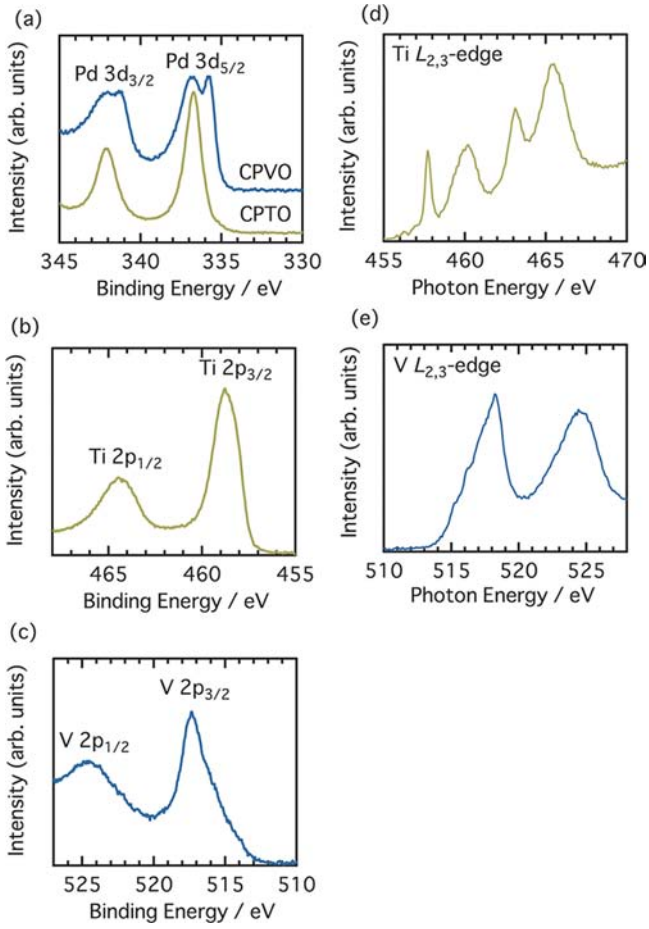

Figure 3. XPS spectra of (a) Pd 3d of $CaPd_3Ti_4O_{12}$ and $CaPd_3V_4O_{12}$, (b) Ti 2p of $CaPd_3Ti_4O_{12}$, (c) V 2p of $CaPd_3V_4O_{12}$. XAS spectra of (d) Ti *L*-edges of $CaPd_3Ti_4O_{12}$ and (e) V *L*-edges of $CaPd_3V_4O_{12}$.

binding energies of Pd $3d_{5/2}$ are about 337 eV for both compounds. This value is very close to that reported for $Pd^{2+}O$ (336.8 eV),[17] revealing that the Pd ions in CPTO and CPVO are divalent. The sharp features at lower binding energies (335.8 and 341.3 eV) observed in the CPVO spectrum are attributed to the nonlocal screening effect, which is observed in hard X-ray photoemission spectra of metallic compounds.[18,19] As further discussed later with the electrical resistivity data, the above-mentioned features derive from the metallic nature of CPVO. The Ti 2p XPS spectrum for CPTO shows that the binding energy of Ti $2p_{3/2}$ is about 458.8 eV (Figure 3b). This value is close to that of $Ti^{4+}O_2$ (458.9 eV),[20] indicating that the Ti is quadrivalent. The spectral shape of the Ti-$L_{2,3}$ edge XAS spectrum is quite similar to that of the isostructural $CaCu_3Ti_4O_{12}$ perovskite,[11] further evidence for quadrivalent Ti in CPTO (Figure 3d). The above spectroscopic analyses reveal that the appropriate valence states are $Ca^{2+}Pd^{2+}{}_3Ti^{4+}{}_4O_{12}$, consistent with the structure refinement result. Figure 3c shows the V 2p XPS spectrum of CPVO. The binding energy of V $2p_{3/2}$ is about 517.4 eV, which is close to the typical value (~517 eV) for V^{4+} ion.[21] The XAS spectrum

dx.doi.org/10.1021/ic3025155 | Inorg. Chem. 2013, 52, 1604−1609

of the V-$L_{2,3}$ edge for CPVO (Figure 3e) also supports the V^{4+} valence state, because its shape is quite similar to that of $V^{4+}O_2$.[22] These spectroscopic analyses demonstrate that the valence states of CPVO are $Ca^{2+}Pd^{2+}{}_3V^{4+}{}_4O_{12}$, as also suggested by the structure refinement result. The above results also exclude significant oxygen deficiency in CPTO and CPVO.

Figure 4 shows the temperature dependence of the electrical resistivity of CPVO. The small value (<10 mΩ cm) and

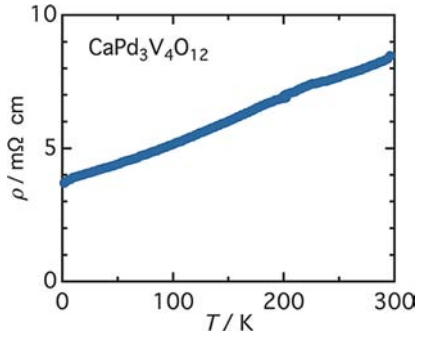

Figure 4. Temperature dependence of the electrical resistivity of $CaPd_3V_4O_{12}$.

positive slope ($d\rho/dT > 0$) indicate that CPVO is metallic over the measured temperature range. A slight anomaly in the vicinity of 220 K probably derives from extrinsic factors such as electrical contact and grain boundary. The nearly linear behavior with temperature for CPVO is similar to that of $CaCu_3V_4O_{12}$.[23] It is unlikely that the metallic conductivity of CPVO can be attributed only to the V 3d and O 2p orbitals, because the V−O−V bond is tightly bent (~145°). This value is slightly larger than but comparable to that in $CaCu_3V_4O_{12}$ (~142°),[23] and much smaller than that of $CaVO_3$ (~160°).[24] Thus, the contribution of the Pd 4d electrons to metallic conduction seems to be essential for CPVO, with these electrons fulfilling a similar role to that of the Cu 3d electrons in $CaCu_3V_4O_{12}$.[23] The electrical resistivity measurement could not be performed for CPTO because of its high resistivity (>10^6 Ω cm at room temperature). The insulating nature of CPTO originates from the absence of carriers. From the spectroscopic analyses, the $3d^0$ electron configuration of the Ti^{4+} ion in CPTO suggests a band-insulating property.

Figure 5 shows the temperature dependences of the magnetic susceptibility (measured in ZFC mode) for CPTO and CPVO. For both compounds, no magnetic transition was observed

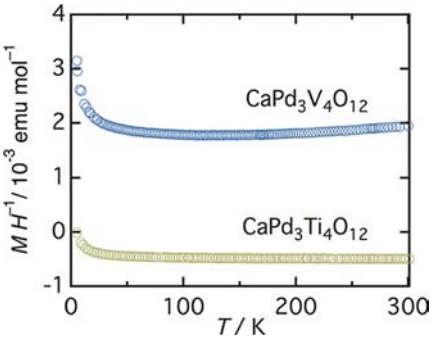

Figure 5. Temperature dependences of the magnetic susceptibility measured in an external field of 1 kOe under ZFC conditions for $CaPd_3Ti_4O_{12}$ and $CaPd_3V_4O_{12}$.

down to 5 K, and there is no significant difference between the FC and ZFC data within the temperature range of the measurement. The temperature-independent negative value of approximately -5×10^{-4} emu/mol for CPTO indicates that CPTO is diamagnetic. Curie−Weiss-like paramagnetic behavior below ~30 K is probably attributed to unidentified paramagnetic impurities; thus we conclude that CPTO is intrinsically diamagnetic. In the case of CPVO, an almost temperature-independent positive value of $\sim 1.8 \times 10^{-3}$ emu/mol was observed. This indicates that CPVO has a Pauli-paramagnetic-like nature, which arises from the conduction electrons. A Curie−Weiss-like paramagnetic upturn below ~30 K was analyzed using the equation: $\chi(T) = \chi_0 + C/(T - \theta)$, where χ_0, C, and θ are the Pauli-paramagnetic-like temperature-independent term, the Curie constant, and the Weiss temperature, respectively. We fitted the data in the temperature range of 5−100 K and found $C = 8.5(2) \times 10^{-3}$ emu K/mol, which corresponds to 0.57% of V^{4+} ions (d^1, $S = 1/2$). Since this fraction is very small, the Curie−Weiss-like paramagnetic property probably originates from the localized spins on grain boundary and/or impurity phases.

The electronic contribution to the specific heat at low temperature was estimated from the C/T vs T^2 plot (Figure 6).

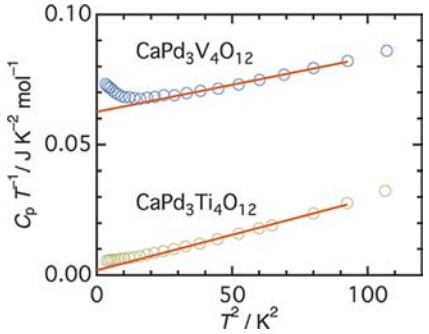

Figure 6. Specific heat data divided by temperature C_p/T as a function of T^2 for $CaPd_3Ti_4O_{12}$ and $CaPd_3V_4O_{12}$. The lines are fits to the data from 5.3 to 9.6 K and extrapolations to lower temperatures.

The data for CPTO and CPVO in the temperature range of 5.3−9.6 K were analyzed using the following equation:

$$\frac{C}{T} = \gamma + \frac{12\pi^4}{5} N_A k_B T^2 \left(\frac{1}{\theta_D^3}\right)$$

where γ, N_A, and θ_D are the Sommerfeld coefficient, the number of atoms, and the Debye temperature, respectively. The values of θ_D (~520 K for CPTO and ~570 K for CPVO) are close to those reported for the isostructural compounds.[25,26] γ values are estimated as almost zero for CPTO and ~60 mJ/mol K^2 for CPVO. The γ value is proportional to the electronic density of states at the Fermi level, $N(E_F)$, so the large γ value for CPVO is consistent with the metallic nature of this material. In contrast, the almost zero γ value for CPTO is as expected for an insulator. The Schottky anomaly below ~4 K for CPVO is because of excitation of the nuclear moment of ^{51}V.

The above experimental results show that the novel perovskite oxides CPTO and CPVO have been successfully synthesized using a high-pressure synthesis method. To the best of our knowledge, this is the first example where Pd^{2+} ions fully occupy a distinct crystallographic site in a perovskite-type structure. Here, we consider the effect of the sizes of the ions in

dx.doi.org/10.1021/ic3025155 | Inorg. Chem. 2013, 52, 1604−1609

Table 2. Lattice Constant a, Ionic Radius of A-site r_A, Difference between Ionic Radii of A- and A'-site Ions Δr_A, and Metal−Oxygen Bond Angles $\angle A'-O-Ti$ and $\angle Ti-O-Ti$ for $AA'_3Ti_4O_{12}$ Perovskites

compound	r_A/Å	Δr_A/Å	$\angle A'-O-Ti$/deg	$\angle Ti-O-Ti$/deg	ref.
$CaPd_3Ti_4O_{12}$	1.34	0.70	107.1(7)	144.93(14)	this work
$CaFe_3Ti_4O_{12}$	1.34	0.70	107.82	144.01	10
$CaCu_3Ti_4O_{12}$	1.34	0.77	108.98	141.33	9
$SrCu_3Ti_4O_{12}$	1.44	0.87	109.18	141.21	27

the A- and A'-sites on the crystal structure of $AA'_3B_4O_{12}$ perovskites. The a-axis lengths for CPTO and CPVO are slightly increased from those of $CaCu_3Ti_4O_{12}$ and $CaCu_3V_4O_{12}$ (by 1.5% and 1.7%, respectively). It is obvious that substitution of the Cu^{2+} ion with the larger Pd^{2+} ion elongates the $A'-O$ bonds, resulting in expansion of the unit cell. This is consistent with the A-site ion size dependence of the unit cell edge length; the a-axis length increases in $ACu_3Ti_4O_{12}$ perovskites from 7.3730 Å (A = Ca^{2+}) to 7.42757 Å (A = Sr^{2+}) and in $ACu_3Ru_4O_{12}$ from 7.41871 Å (A = Ca^{2+}) to 7.44754 Å (A = Sr^{2+}).[27,28] This indicates that the unit cell volume is dependent on both the $A-O$ and $A'-O$ bond lengths. The metal−oxygen bond angles are largely controlled by the difference between the A- and A'-site ion radii.[13] Table 2 lists the ionic radii of A-site ions r_A, the difference between A- and A'-site ion radii Δr_A, and the metal−oxygen bond angles $\angle A'-O-Ti$ and $\angle Ti-O-Ti$ for $A^{2+}A'^{2+}{}_3Ti^{4+}{}_4O_{12}$ (A = Ca and Sr, A' = Cu, Fe, and Pd) perovskites. Note that the $\angle A'-O-Ti$ and $\angle Ti-O-Ti$ bond angles, respectively, decrease and increase with increasing Δr_A. This means that these two bond angles become closer to those of a cubic ABO_3 perovskite (90° and 180° for $\angle A-O-B$ and $\angle B-O-B$, respectively) as Δr_A decreases. The ionic radius of the A-site ion itself hardly affects these bond angles, which is the same way as the lights pointed out in $ACu_3Ru_4O_{12}$ (A = Na, Ca, Sr, La, and Nd) perovskites.[28] The above situation differs from the general trend for simple ABO_3 perovskites, where the ionic radius of the A-site ion dominates the $\angle A-O-B$ and $\angle B-O-B$ bond angles. Instead, both the ionic radii of A- and A'-site ions affect the bond angles in $A^{2+}A'^{2+}{}_3Ti^{4+}{}_4O_{12}$ perovskites.

The electronic properties of CPVO demonstrate that the substitution of Pd^{2+} for Cu^{2+} induces drastic changes in electronic structure. The γ value almost doubles from ∼30 mJ/mol K^2 for $CaCu_3V_4O_{12}$ to ∼60 mJ/mol K^2 for CPVO, and the Pauli-paramagnetic susceptibility also increases from $\sim 1 \times 10^{-3}$ emu/mol for $CaCu_3V_4O_{12}$ to $\sim 1.8 \times 10^{-3}$ emu/mol for CPVO. Since these parameters are proportional to $N(E_F)$ for metallic band structure, the $N(E_F)$ of CPVO is estimated to be about twice that of $CaCu_3V_4O_{12}$. The increase in $N(E_F)$ probably originates from the contribution of A'-site ions (Cu^{2+} and Pd^{2+}) to the band structure near the Fermi level, suggesting that the A'-site ions play a crucial role in the metallic conduction of these V-based perovskites.

CONCLUSIONS

We have synthesized the novel $AA'_3B_4O_{12}$-type perovskites $CaPd_3Ti_4O_{12}$ and $CaPd_3V_4O_{12}$ under high-pressure, high-temperature conditions (15 GPa and 1000 °C), and their magnetic and electrical transport properties have been revealed. The substitution of Cu^{2+} with Pd^{2+} induces drastic changes in the parameters that characterize the electronic structures. A probable explanation for the differences between electronic properties of $CaCu_3V_4O_{12}$ and $CaPd_3V_4O_{12}$ is that the electronic structures in the vicinity of the Fermi level are sensitive to the A'-site ions.

ASSOCIATED CONTENT

Supporting Information

Crystallographic data of $CaPd_3Ti_4O_{12}$ and $CaPd_3V_4O_{12}$ (CIF). This material is available free of charge via the Internet at http://pubs.acs.org.

AUTHOR INFORMATION

Corresponding Author

*E-mail: i-yamada@21c.osakafu-u.ac.jp. Phone: +81-72-254-9817.

Present Address

#Deutsches Elektronen Synchrotron (DESY), 22607 Hamburg, Germany.

Notes

The authors declare no competing financial interest.

ACKNOWLEDGMENTS

We appreciate our fruitful discussions with Masahiko Tsujimoto. The synchrotron radiation experiments were performed at SPring-8 with the approval of the Japan Synchrotron Radiation Research Institute (Proposal Nos. 2009B1322, 2011B1009, and 2012A1660). The physical property measurements were performed using the facilities of the Institute for Solid State Physics, University of Tokyo. This work was partly supported by JST-PRESTO and by the Grant-in-Aid for Young Scientist (B) No. 21750062.

REFERENCES

(1) Orosel, D.; Jansen, M. *Z. Anorg. Allg. Chem.* **2006**, *632*, 1131−1133.

(2) Martínez-Lope, M. J.; Retuerto, M.; Alonso, J. A.; Sánchez-Benítez, J.; Fernández-Díaz, M. T. *Dalton Trans.* **2011**, *40*, 4599−4604.

(3) Inaguma, Y.; Tanaka, K.; Tsuchiya, T.; Mori, D.; Katsumata, T.; Ohba, T.; Hiraki, K.; Takahashi, T.; Saitoh, H. *J. Am. Chem. Soc.* **2011**, *133*, 16920−16929.

(4) Kim, S. J.; Lemaux, S.; Demazeau, G.; Kim, J. Y.; Choy, J. H. *J. Am. Chem. Soc.* **2001**, *123*, 10413−10414.

(5) The crystal structure is drawn by using VESTA. Momma, K.; Izumi, F. *J. Appl. Crystallogr.* **2008**, *41*, 653−658.

(6) Deschanvres, A.; Raveau, B.; Tollermer, F. *Bull. Soc. Chim. Fr.* **1967**, *11*, 4077−4078.

(7) Bochu, B.; Chenavas, J.; Joubert, J. C.; Marezio, M. *J. Solid State Chem.* **1974**, *11*, 88−93.

(8) Subramanian, M. A.; Dong, Li.; Duan, N.; Reisner, B. A.; Sleight, A. W. *J. Solid State Chem.* **2000**, *151*, 323−325.

(9) Subramanian, M. A.; Sleight, A. W. *Solid State Sci.* **2002**, *4*, 347−351.

(10) Leinenweber, K.; Linton, J.; Navrotsky, A.; Fei, Y.; Parise, J. B. *Phys. Chem. Miner.* **1995**, *22*, 251−258.

(11) Long, Y.; Saito, T.; Mizumaki, M.; Agui, A.; Shimakawa, Y. *J. Am. Chem. Soc.* **2009**, *131*, 16244−16247.

(12) Izumi, F.; Momma, K. *Solid State Phenom.* **2007**, *130*, 15−20.

(13) Shannon, R. D. *Acta Crystallogr., Sect. A* **1976**, *32*, 751−767.

(14) Sanchez-Benitez, J.; Alonso, J. A.; Martinez-Lope, M. J.; Casais, M. T.; Martinez, J. L.; de Andres, A.; Fernandez-Diaz, M. T. *Chem. Mater.* **2003**, *15*, 2193−2200.
(15) Avdeev, M.; Nalbandyan, V. B. *Inorg. Chem.* **2006**, *45*, 2217−2220.
(16) (a) Brown, I. D.; Altermatt, D. *Acta Crystallogr.* **1985**, *B41*, 244−247. (b) The BVS were calculated using the following parameters: b_0 = 0.37 for all atoms, r_0 = 1.967 for Ca^{2+}, r_0 = 1.792 for Pd^{2+}, r_0 = 1.815 for Ti^{4+}, and r_0 = 1.784 for V^{4+}.
(17) Brun, M.; Berthet, A.; Bertolini, J. C. *J. Electron Spectrosc. Relat. Phenom.* **1999**, *104*, 55−60.
(18) Taguchi, M.; Chainani, A.; Horiba, K.; Takata, Y.; Yabashi, M.; Tamasaku, K.; Nishino, Y.; Miwa, D.; Ishikawa, T.; Takeuchi, T.; Yamamoto, K.; Matsunami, M.; Shin, S.; Yokoya, T.; Ikenaga, E.; Kobayashi, K.; Mochiku, T.; Hirata, K.; Hori, J.; Ishii, K.; Nakamura, F.; Suzuki, T. *Phys. Rev. Lett.* **2005**, *95*, 177002.
(19) Sudayama, T.; Wakisaka, Y.; Takubo, K.; Mizokawa, T.; Kobayashi, W.; Terasaki, I.; Tanaka, S.; Maeno, Y.; Arita, M.; Namatame, H.; Taniguchi, M. *Phys. Rev. B* **2009**, *80*, 075113.
(20) Demri, B.; HageAli, M.; Moritz, M.; Kahn, J. L.; Muster, D. *Appl. Surf. Sci.* **1997**, *108*, 245−249.
(21) Sawatzky, G. A.; Post, D. *Phys. Rev. B* **1979**, *20*, 1546−1555.
(22) Ruzmetov, D.; Senanayake, S. D.; Ramanathan, S. *Phys. Rev. B* **2007**, *75*, 195102.
(23) Shiraki, H.; Saito, T.; Azuma, M.; Shimakawa, Y. *J. Phys. Soc. Jpn.* **2008**, *77*, 064705.
(24) Falcon, H.; Alonso, J. A.; Casais, M. T.; Martinez-Lope, M. J.; Sanchez-Benitez, J. *J. Solid State Chem.* **2004**, *177*, 3099−3104.
(25) Tanaka, S.; Shimazui, N.; Takatsu, H.; Yonezawa, S.; Maeno, Y. *J. Phys. Soc. Jpn.* **2009**, *78*, 024706.
(26) Yamada, I.; Ishiwata, S.; Terasaki, I.; Azuma, M.; Shimakawa, Y.; Takano, M. *Chem. Mater.* **2010**, *22*, 5328−5532.
(27) Li, J.; Subramanian, M. A.; Rosenfeld, H. D.; Jones, C. Y.; Toby, B. H.; Sleight, A. W. *Chem. Mater.* **2004**, *16*, 5223−5225.
(28) Ebbinghaus, S. G.; Weidenkaff, A.; Cava, R. J. *J. Solid State Chem.* **2002**, *167*, 126−136.

dx.doi.org/10.1021/ic3025155 | *Inorg. Chem.* 2013, 52, 1604−1609